Performance Evaluation of IEEE 802.15.4-2011 IR-UWB System with Enhanced Modulation Scheme

Conference Paper · September 2015

DOI: 10.4108/eai.28-9-2015.2261507

5 authors, including:

Tuomas Paso
University of Oulu
25 PUBLICATIONS **138** CITATIONS
SEE PROFILE

Jussi Haapola
University of Oulu
60 PUBLICATIONS **1,095** CITATIONS
SEE PROFILE

Matti Hämäläinen
University of Oulu
220 PUBLICATIONS **3,126** CITATIONS
SEE PROFILE

Jari Iinatti
University of Oulu
268 PUBLICATIONS **4,182** CITATIONS
SEE PROFILE

Performance Evaluation of IEEE 802.15.4-2011 IR-UWB System with Enhanced Modulation Scheme

Tuomas Paso[1], Ville Niemelä[1], Jussi Haapola[1,2], Matti Hämäläinen[1], Jari Iinatti[1]
[1]University of Oulu, Centre for Wireless Communications, P.O. Box 4500, FI-90014 University of Oulu, Finland
[2]University of Oulu Research Institute in Japan – CWC Nippon (KK, Ltd.), Yokohama, Japan
{tuomas.paso, ville.niemela, jussi.haapola, matti.hamalainen, jari.iinatti}@ee.oulu.fi

ABSTRACT
In this paper, we propose and analyze an enhanced modulation scheme for impulse radio ultra wideband (IR-UWB) communications based on the IEEE Std. 802.15.4-2011. Currently, the pulse position modulation as utilized in the standard wastes 50% of the possible transmission time, but with suitable enhancement it can be taken into effective use. The advantages of the proposed improvement include data rate increase and enhanced resilience against multi-user interference and poor channel conditions. We provide IR-UWB receivers' performance evaluations and comparisons by simulations in a real measured and modelled body-to-external channel model with different modulations. In addition, we provide analytical system level results of the IEEE Std. 802.15.4-2011 based communication system. We demonstrate on a network level how the proper selection of the IR-UWB modulation can increase the successful traffic volume up to 74%. All this is performed with backward compatibility to the aforementioned standard and, moreover, it can be utilized in the IEEE Std. 802.15.6-2012 IR-UWB communications, too.

Categories and Subject Descriptors
C.2.2 [**Computer – Communication Networks**]: Network Protocols; C.2.2 [**Computer – Communication Networks**]: Network Architecture and Design – Wireless Communication.

General Terms
Performance, Design, Reliability, Theory.

Keywords
Energy detector, IEEE Std. 802.15.4-2011, IEEE Std. 802.15.6-2012, hospital radio channel model, modulation, rake receivers, Slotted-ALOHA, ultra wideband.

1. INTRODUCTION
The first impulse radio ultra wideband (IR-UWB) standard, IEEE 802.15.4a, was published in 2007. Currently it is incorporated in the IEEE Std. 802.15.4-2011, and it is targeted for low power and low-complexity short-range wireless personal area networks (WPANs) [1]. In February 2012, another standard including IR-UWB was published. The IEEE Std. 802.15.6-2012 is targeted for wireless body area networks (WBANs) [2] and it can be used, for example, in health monitoring through wireless sensor networks, in a similar way as the earlier published WPAN standard.

A conference article [3] was published in 2011 proposing novel enhancements concerning physical layer (PHY) modulation scheme of the IEEE Std. 802.15.4-2011. This paper provides system level analysis of the proposal, demonstrating a considerable increase in successful traffic volume at a network level. Additionally, this paper offers more comprehensive PHY layer simulation results than the ones presented in [3]. The system models utilized are based on the definitions of the IEEE Std. 802.15.4-2011. We have also included in the transceiver system few other modulation methods than the two defined in the standard to provide more extensive insight of the possibilities. Moreover, system level evaluations of the receiver performances with different modulations are provided for the first time. Finally, this paper extends how the idea can be covered also for the IEEE Std. 802.15.6-2012 [2].

A transceiver system can benefit from the proposed idea in numerous ways, yet retaining compatibility not only with the IEEE Std. 802.15.4-2011 but also with the latest WBAN standard IEEE Std. 802.15.6-2012. In both standards, IR-UWB is used and therefore, any system following the standards' definitions can improve the performance and adaptability by utilizing the method thoroughly analyzed in this paper.

The rest of the paper is organized as follows. The idea of the improvement is represented in Section 2. In Section 3, the system model utilized to demonstrate the proposed improvement is presented. Section 4 presents the analytical results by simulations and Section 5 concludes the article.

2. ENHANCEMENT FOR THE IR-UWB MODULATION SCHEME

2.1 IEEE Std. 802.15.4-2011 UWB Symbol Structure and Modulations
Figure 1 illustrates the symbol structure of a UWB signal, as defined in the IEEE Std. 802.15.4-2011. The symbol is divided into four quarters; each quarter is further divided into 2, 8 or 32 time-hopping positions. [1]

The standard defines two binary modulation methods for the UWB: burst (pulse) position modulation (BPM) and binary phase-shift keying (BPSK). These modulation methods are executed in a consecutive manner in the sense that BPSK cannot be used alone but should be used additionally with BPM. Generally, an information bit is position modulated and the additional phase modulated bit is dedicated for redundant convolutional channel

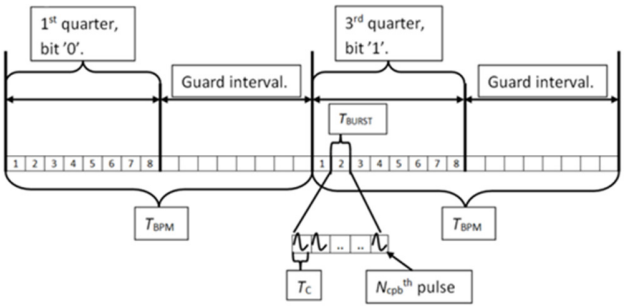

Figure 1. UWB symbol structure in IEEE Std. 802.15.4-2011.

coded bit. In some options though, the phase modulated bit can be an information bit as well, i.e., two information bits are transmitted in one symbol, i.e., in a burst. The benefit of this type of modulation is that receiving and demodulating a burst can be done either in coherent or non-coherent methods yet retaining exactly the same information. In such a way coherent receivers can improve their performance by decoding the convolutional coding or non-coherent receivers can gain in simplicity. [1]

This type of modulation method has also drawbacks. The first one is caused by the nature of position modulation. Having different instants for binary transmissions inevitably means that 50% of the transmission time is unused. The second drawback is the combination of BPM and BPSK. Since a burst can also be phase modulated, the position demodulation, in practice, is done in a non-coherent manner. However, coherent detection would have better performance than non-coherent detection. The next section represents an alternative way to modulate the signal yet retaining the same symbol structure as defined in the IEEE Std. 802.15.4-2011. Utilizing the proposed method can still be done using a modulation method defined in the standard but it can also be done using other known modulation techniques suitable for IR communications. Modulating UWB signal in another way provides a few additional advantages.

2.2 The Proposed Enhancement

The proposed modification can be summarized in one phrase; bypassing the position modulation [3]. Utilizing another modulation than the BPM opens a whole new perspective yet retaining compatibility with the existing standard. According to the proposal, the unused time can be taken in use by doubling the available burst positions. This provides an option to let the same user to transmit during both of the two dedicated hopping positions within a single symbol which would, at most, double the physical layer data rate. Since the guard intervals exist inside the symbol, the inter-symbol-interference (ISI) can be ignored, at least with the timing-related parameters leading to long symbol duration when compared to the maximum multipath delays.

The proposed scheme can be utilized also with transmitted reference type receivers or extend it to *M*-ary signaling. In transmitted reference signaling, the information is typically constructed of two separate transmissions [4]. Other modulations well-known in IR-UWB communications besides the PPM and PSK are pulse amplitude modulation (PAM), on-off-keying (OOK), and pulse shape modulation (PSM).

To the best of our knowledge, there has not been any proposition in UWB communication than in [3] relating to bypassing PPM and utilizing some other modulation instead. The closest one, [5], states that binary-orthogonal-coded OOK signaling is equivalent to binary-orthogonal PPM. The same is also mentioned in the Annex C of the IEEE Std. 802.15.6-2012 [2], in which the used *M*-bit grouping in OOK is coinciding with binary PPM.

Furthermore, the proposed enhancement can be adopted into the IEEE Std. 802.15.6-2012 based systems as well. The symbol structure of the IR-UWB definitions of both of the standards is very similar. However, the difference is that the guard intervals have been dropped out in IEEE Std. 802.15.6-2012, and there is a fixed number, 32, of possible pulse positions. The modulation methods for the IR-UWB are OOK and differential binary PSK; the first one defined to be used in the mandatory mode. In OOK case, the symbol is divided in two halves due to the symbol mapping, in which one information bit is expressed with a two-bit code word. As is explained in Annex C of the IEEE Std. 802.15.6-2012 [2], two-bit grouper and half rate symbol mapper coincides with binary PPM. Therefore, the enhancement, presented in [3], can be used also in a system built according to the IEEE Std. 802.15.6-2012 IR-UWB definitions with all the benefits explained in the previous section.

2.3 Studies for Increasing Data Rate in UWB

In order to increase data rates in impulse radio UWB, there exist many studies of combining modulation methods in single transmission. What comes to the idea presented in [3], the modulation combining is particularly interesting because it can be seen as the opposite action to the proposed partitioning of the PPM signaling. Different proposed combinations include, at least, PSM-PPM in [6], PAM-PSM in [7], OOK-PSM in [8] and the aforementioned BPM-BPSK used in the IEEE Std. 802.15.4-2011 [1]. Another interesting proposed modulation "combination" was presented in [9], called binary pulse shape frequency shift keying. Despite the name, it is a modification of pulse shape modulation, in which, instead of orthogonal pulses traditionally used in PSM, it uses pulses that are located in different frequencies indicating different data. Any of these can be used for increasing data rate, especially if *M*-ary signaling is added also. However, the proposal in [3] reaches towards low-cost and low-complexity implementation; the core thoughts, for example, in the two IEEE standards concerning IR-UWB. Additionally, this proposal provides an opportunity for improved adaptability to different demands of a system and yet, it is not exclusive of using the combination of modulations.

3. SYSTEM MODEL

In order to make the proposal work also on a system level, a novel idea of informing the receivers of the used modulation methods is performed by adding an extra field in the PHY header [10]. However, this paper is concentrating on i) the performance evaluations of the IR-UWB receivers and ii) the effects of the proposal on the system level performance regarding medium access control (MAC) layer. Therefore the system model of this paper is divided into two separate but dependent entities: PHY layer and MAC layer.

The PHY layer evaluation is executed with transmitter-receiver pairs according to the IR-UWB PHY layer definitions of the IEEE Std. 802.15.4-2011 [1]. Additionally, this model includes the proposed improvements from [3] and with additional receiver structures which are described in details in [11]. When simulating and evaluating the performances of different receivers in the PHY simulation model, we assume perfect synchronization between the transmitter and receivers, as is usual in the literature, and no additional interference is considered either, in addition to a realistic channel model. The differences in the performances of

the PHY simulations are due to chosen receiver structure and modulation methods.

The used PHY and MAC parameters are presented in Table 1. Symbol length is 1025 ns leading into 256 ns guard intervals. Compared to the maximum multipath delays of the used channel model, approximately 30 ns, it is more than sufficient to prevent ISI. Reed-Solomon encoding and its impact on the performance is included in the bit error ratio (BER) curves presented later.

In the MAC layer evaluation, the overall throughput of the system is analyzed with the effects of the PHY layer modulations. It is done by modeling the used slotted ALOHA (S-ALOHA, defined in the IEEE Std. 802.15.4-2011 for IR-UWB) network as a homogenous finite Markov process using a known S-ALOHA model [12,13]. On top of this, the overhead caused by the standard's requirements for successful communications using S-ALOHA is calculated and presented. The output of the MAC simulation model presents the total throughput of a system built according to the IEEE Std. 802.15.4-2011 definitions. Thus, the system level comparisons with different modulation methods can be made and the overhead caused by the standard's definitions is visible also.

The overall system model consists of a hub collecting all the measured data (from separate sensors located around the body, for example, with the IEEE Std. 802.15.6-2012 system). The data is being transmitted to a room access point, located 2 meters from the body, with an IEEE Std. 802.15.4-2011 UWB transceiver system and a modified version of it with other modulations than the standard defines. On the system level inspections, the number of the body hubs is increased to describe a real scenario, for example, several patients in a hospital room or in an emergency evacuation area with each one carrying a body vitals' measurement and transmitting unit.

For more detailed information about the standard's UWB definitions, reader is referred to [1]. [14-16] provide overviews with analysis of the standard [1].

3.1 Transmitted Waveform

The transmitted UWB waveform during the k^{th} symbol interval is expressed as [1]

$$x^{(k)}(t) = \left[1 - 2g_1^{(k)}\right] \sum_{n=1}^{N_{\text{cpb}}} \left[1 - 2s_{n+kN_{\text{cpb}}}\right] \times p\left(t - g_0^{(k)} T_{\text{BPM}} - h^{(k)} T_{\text{burst}} - nT_{\text{c}}\right), \quad (1)$$

where $g_0^{(k)}$ is a position modulated bit and $g_1^{(k)}$ is a phase modulated bit. N_{cpb} stands for the number of pulses per burst. Sequence $s_{n+kN_{\text{cpb}}} \in \{0,1\}$, $n = 0, 1, \ldots, N_{\text{cpb}}-1$ is the scrambling code used in the k^{th} interval and $h^{(k)}$ is the k^{th} burst hopping position defined also by the scrambler. $p(t)$ is the transmitted pulse waveform at the antenna input being either the 5th Gaussian derivative pulse (PSM) or the 6th Gaussian derivative pulse (PSM and all other modulations). T_{BPM} is the half length of a symbol defining the position of the burst within the symbol, T_{burst} is the length of a burst and T_{c} is the length of a pulse. The symbol structure is presented in Figure 1. [1]

Utilizing the proposal presented in [3], the transmission of two bursts is occurring in both symbol quarters, in the first and in the third one, according to the time varying hopping code, $h^{(k)}$. This leads to twice as high PHY layer data rate compared to the standard's BPM. Since there are two separate transmissions during one symbol interval, $g_0^{(k)}$ needs to be modified. It is done

Table 1. Main PHY and MAC parameters

Symbol	Value
Data rate	850 kbps[1]
N_{cph}	4 pulses[1]
aMaxMACPayloadSize	944 bits[1]
$\text{SlotDuration}_{\text{ALOHA}}$	1286 symbols[2]
δ_{beacon}	0.9895/0.9936[2]
N	0-60[2]
p_0	0.036/0.022[2]
p_{r}	0.036/0.022[2]

[1]IEEE Std. 802.15.4-2011 defined, [2]user-defined

by replacing $g_0^{(k)}$ in (1) by $g_{0_{i+1}}^{(k)}$ as

$$g_{0_{i+1}}^{(k)} = \begin{cases} 0, i = 0, \\ 1, i = 1, \end{cases} \quad (2)$$

where $i + 1$ presents either the first or the second transmitted bit, depending on the value of i, within the k^{th} symbol interval. Similarly, $g_1^{(k)}$ in (1) is replaced by $g_{1_{i+1}}^{(k)}$ as

$$g_{1_{i+1}}^{(k)} = \begin{cases} 0, i = 0, \\ 1, i = 1, \end{cases} \quad (3)$$

where $i + 1$ presents either the first or the second transmitted bit.

By modifying the variable $g_0^{(k)}$, its meaning changes as well. Initially it was used as a delay marker for the purpose of position modulation and there existed only one transmission within a symbol interval. In the proposed system, the variable can have both values 0 and 1 during one symbol interval leading into two separate transmissions.

In this paper, the signal is modulated with four different binary modulations: PSK, PSM, PPM and OOK. For other than the PPM (BPM), the transmission scheme is according to the proposed technique, explained in Section 2.2 and in (1), (2) and (3). With PPM, the transmission is directly according to the original definitions of the standard. With PSK, the transmitted waveform is also according to the standard definitions, but now without the position modulated delay component $g_0^{(k)} \times T_{\text{BPM}}$. Therefore, there are (or can be) two impulse transmissions within one symbol. In PSM modulation, the transmitted burst is constructed of the 6th Gaussian derivative pulses, if the data bit is '1' and the 5th Gaussian derivative pulses, if the data bit is '0'. For OOK, there is a transmission for data bit '1' and no transmission for data bit '0'. Except the modulations, the signaling is following the standard definitions with the same symbol structure, time-hopping ruling, Reed-Solomon encoding and burst construction.

3.2 Channel Model

The channel model used here is based on a measurement campaign in a real hospital environment [17]. It is a body-to-external channel model, from the center of a body to the top of a 2-meter pole with link distance of 2 meters. Channel models based on the same measurement campaign has been used earlier in research as well [18-19].

In the PHY simulations, there are 100 channel realizations generated and the receiver performance results are averaged over those. Considering the total number of bits of 2.5×10^6, it means

that 2.5×10^4 bits is transmitted over each channel realization. The power distribution of the taps of a single channel realization is always normalized to one.

3.3 MAC Layer Analysis Model

For the MAC layer analysis, we consider an S-ALOHA network with N terminals sharing one channel for transmission to one receiver. During any time slot each terminal will be in any of three states: the origination state (O) when a terminal has no packet to transmit or a new packet has just arrived while the terminal is waiting for the next time slot; the transmission state (T) when a terminal is transmitting a packet (successfully or not); and the retransmission state (R), where terminal is waiting for retransmission after an unsuccessful transmission attempt. Terminal is referred to as an O-, T-, or R-terminal depending on its state. While a terminal has a packet to transmit, it is assumed that the packet generating process comes to a halt. [12]

The S-ALOHA network can be described as a homogeneous finite Markov process with N+1 possible states (0,1,...,N), corresponding to the number of R-terminals at the end of a time slot. The possible transitions for an individual terminal are shown in Figure 2. State changes can occur either at the end or beginning of a time slot. The probability for the change from O to T will be denoted p_0, which is the packet generation rate. The probability for the change from R to T is termed p_r (retransmission rate). [12]

Assuming i ($0 \le i \le N$) T-terminals transmitting in one time slot, the probability that excatly one of them will transit to O and the rest to R will be denoted q_i (success probability). Naturally $q_0 = 0$ and if no channel error occurs, $q_1 = 1$. In this paper capture effect is not considered, therefore other values for q_i are zero (i.e. transmissions are not successful if there are two or more simultaneous transmissions). [12]

Let $\pi_{n,m}$ denote the state transition probability that the network will move from state n to m in one step (from the end of one time slot to the end of the next one). We get three types of transitions [12]:

i) The state decreases by more than one. Since only one packet can be successfully decoded at the same time, this is not possible.

ii) The state decreseas by one. This will happen when $n > 0$ and one R-terminal changes into state T (successful transmission).

iii) The state moves to $m \ge n$. This will happen either with probability $q_{i+m-n+1}$ if $m - n + 1$ O-terminals and i, $0 \le i \le n$, R-terminals change into state T (one packet successful); or with probability $1 - q_{i+m-n+1}$ if $m - n$ O-terminals and i, $0 \le i \le n$, R-terminals change into state T (no successful transmissions).

Assuming that the terminals are independent, we get the state transition probabilities [12]

$$\pi_{n.m} = \begin{cases} 0, m < n-1 \\ (1-p_0)^{N-n}\sum_{i=1}^{n}\binom{n}{i}p_r^i(1-p_r)^{n-1}q_i, m = n-1 \\ \left.\begin{array}{c}\binom{N-n}{N-m}(1-p_0)^{N-m-1}p_0^{m-n}\sum_{i=0}^{n}\binom{n}{i} \\ \cdot(1-p_r)^{n-1}p_r[(1-p_0) \\ \cdot(1-q_{i+m-n}) + \frac{N-m}{m-n+1}p_0 \\ \cdot q_{i+m-n+1}]\end{array}\right\}, m \ge n. \end{cases} \quad (4)$$

From (4) the equilibrium state occupation probabilities can be calculated as [12]

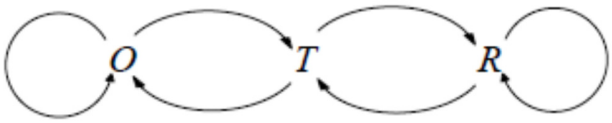

Figure 2. State transitions for an individual terminal in homogeneous finite Markov process.

$$\pi_n^* = \frac{1}{\pi_{n,n-1}}\left(\pi_{n-1}^* - \sum_{i=0}^{n-1}\pi_i^*\pi_{i,n-1}\right), \quad (5)$$

and after normalizing [12]

$$\pi_n = \frac{\pi_n^*}{\sum_{i=0}^{N}\pi_i^*}. \quad (6)$$

The expected throughput of the network in state n is [12]

$$f_n = \sum_{k=0}^{N-n}\binom{N-n}{N-n-k}p_0^k(1-p_0)^{N-n-k}\sum_{i=0}^{n}\binom{n}{i}p_r^i(1-p_r)^{n-i}q_{i+k}. \quad (7)$$

The overall mean throughput is [12]

$$f = \sum_{i=0}^{N}\pi_i f_i, \quad (8)$$

where f_i is the expected throughput of the system in state i. The utilized Markov process is presented in more details in [12], and it is further developed in [13] to cover a special case related to capture effect phenomenon. In addition, similar analysis based on [20] provides converging results.

Finally, when the standard's definitions and the effect of the channel is taken into account, the throughput, S_{out}, of the system as a function of number of transmitting terminals, N, is calculated as

$$S_{out} = f \times PER \times \delta_{\text{total}}, \quad (9)$$

where PER is packet error rate and δ_{total} is the total overhead caused by the standard's definitions. PER is a transformation of BER according to [21] and it is independent of the f_i. The BER values of different modulations are obtained from the PHY layer simulations with given E_b/N_0, where E_b states for energy of a bit, i.e., energy over one transmitted burst and N_0 is zero mean Gaussian noise. δ_{total} is calculated as

$$\delta_{\text{total}} = \frac{aMaxMACPayloadSize}{SlotDuration_{\text{ALOHA}}} \times \delta_{\text{beacon}}, \quad (10)$$

where $aMaxMACPayloadSize$ is a standard defined parameter in bits, $SlotDuration_{\text{ALOHA}}$ is the required slot duration in symbols enabling transmission of the maximum sized packet and its acknowledgement with UWB PHY, and δ_{beacon} is the overhead coefficient in which the beacon transmission is occupying one ALOHA slot in each superframe. The standard defined and selected parameters are given in Table 1. Note, that for some variables, there are two values defined. The first values are used when the standard is followed directly. The second values are used when the PPM is bypassed enabling the transmission of two data bits per one symbol. When some other modulation is used instead of the PPM, the overhead is calculated by allowing the two-bit transmission per symbol only for the MAC headers and PHY payload. By this way, the number of symbols during one Aloha slot is significantly reduced but yet, the same number of bits is transmitted. Thus, the superframe structure of the standard remains the same. Reducing the number of symbols will also affect the per slot packet generating rate, p_0.

The p_0 has been calculated using information rate demands from [22]. We are considering five different vital signs measured from

the body (electrocardiography, electroencephalography, respiratory and heart rate, body temperature). The total information rate is therefore 20680 bps per patient. Separately calculated it requires 24 transmitted packets per second to transfer all the measured data. The packet retransmission rate, p_r, on the other hand, is defined to be the same as p_0 since we do not have to optimize the network performance to any particular number of terminals and this provides also comparable results to theoretical curves.

For the selection of BER values for different modulations, multiple E_b/N_0 values are used to evaluate the total performance of a communication system, i.e., a system level performance. Another limiting factor is the standard defined Reed-Solomon error correction ability; 4 bits per every 330 bit block [1]. Therefore the BER value of each modulation needs to be lower than 1.2×10^{-2}. The packet is lost if any of the blocks in the packet is uncorrectable [14]. In addition, when the BER is lower than 1.7×10^{-3}, practically all the packets are correctly received (as shown in the results).

4. RESULTS

Both the PHY and the MAC layer simulations have been performed in Matlab®. In PHY simulations, 2.5×10^6 bits per each E_b/N_0 value were simulated. Figure 3 presents the obtained BER as a function of E_b/N_0. Considering the E_b/N_0 and the used body-to-external channel model, we estimated that the maximum signal-to-noise ratio at the receiver located 2 meters distant from the transmitter is approximately 26 dB when IR-UWB signal is transmitted with the effective isotropic radiated power limitation of –41.3 dBm/MHz.

MAC layer simulation results present the performance of the communication system based on the IEEE Std. 802.15.4-2011 utilizing IR-UWB PHY and S-ALOHA. Figure 4 presents throughput with different modulations with fixed E_b/N_0=14 dB as a function of number of terminals (body hubs). Third dimension is added to Figure 5, where system performance is presented as a function of number of terminals and different E_b/N_0 values. The following sections discuss the result details.

4.1 PHY Layer Simulation Results

Figure 3 present BER curves in the measured IR-UWB body-to-external channel model with four different modulations and five different receiver structures. Utilized receiver structures are energy detector (ED) and 20 finger p-rake. That many fingers can still be considered reasonable but yet offering good performance characteristics. In addition, results with PPM and PSK modulations in AWGN channel have been added as reference in order to evaluate the effect of the channel on the results.

On a BER level of 10^{-2}, being slightly better than the requirement for the Reed-Solomon decoding, PSK has the best performance. When comparing it to PSM, there is approximately a 3 dB difference, as there is in the theoretical curves in AWGN channel presented in [23]. The orthogonal non-coherent receiver with PPM is approximately 0.5 dB worse and the PPM-ED receiver approximately 1.5 dB worse than the PSM receiver. Clearly the worst performance is achieved with OOK-ED receiver, since the difference to PPM-ED is approximately 4 dB.

On a BER level of 10^{-3}, there are some changes. PSK has still the best performance but the second best performance is now with PPM-ED receiver. The difference is 3.5 dB as is the difference between the two ED receivers with PPM and OOK, OOK-ED

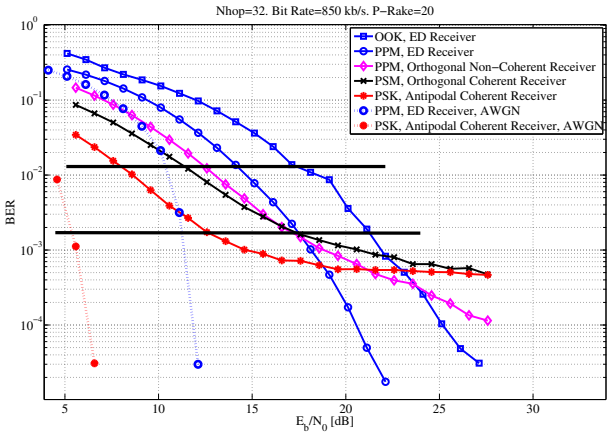

Figure 3. Receiver performances in the body area network channel.

receiver being the worse performing receiver on a BER level of 10^{-3}. Both PSM coherent and PPM non-coherent receiver have fallen behind of the PPM-ED receiver and their performance curves have started to saturate slowly also. The comparison of the receivers below the BER level of 10^{-3} (1.7×10^{-3} to be exact) is unnecessary since the throughput will reach its maximum as will be shown in Figure 4. Since all the receiver types achieve the BER level 1.7×10^{-3} with smaller E_b/N_0 than the estimated maximum of 26 dB, it offers some power saving possibilities for maximizing the battery life. Note also that with ED receivers, increasing the transmitted burst length will also increase the effect of noise to some extent. Therefore with very short burst lengths (the shortest burst lengths lead to short symbols as well) the BER performance would be better as long as, in real channels, ISI is avoided.

4.2 MAC layer results

Throughput for S-ALOHA with different modulations as a function of number of terminals is presented in Figure 4. The utilized E_b/N_0 is fixed to 14 dB. The theoretical S-ALOHA curves with inter-arrival rates, following geometric and exponential distributions achieve their maximum throughput of 0.368 when the number of terminals is 27. Since offered load G can be expressed as $G = Np_0$, this corresponds to offered load of 1 Erlang. The same theoretical results are obtained by utilizing the S-ALOHA model presented in Section 3.3. When overhead caused by the IEEE Std. 802.15.4-2011 is included in the utilized S-ALOHA model, performance of the communication system is significantly decreased. Maximum throughput is now approximately 0.28, which corresponds to 27 % decrease when compared to theoretical results without the overhead (total overhead δ_{total} defined in Section 3.3. is 0.73). When observing the throughputs with different modulations, it can be seen that PSK achieves exactly the same throughput as theoretical S-ALOHA with overhead. The result is expected, since the BER for PSK with E_b/N_0=14 dB is significantly under the threshold value required for perfect correction in the Reed-Solomon decoding phase, and therefore with PSK there are no packet errors. The performance of PSM and non-coherent PPM are slightly decreased from the PSK, yielding approximately the maximum throughputs of 0.25 and 0.22, respectively.

Furthermore, the throughputs of PPM-ED and OOK-ED receivers are zero. This was also expected, since the BER for the PPM-ED with E_b/N_0=14 dB is not quite on the required BER threshold and

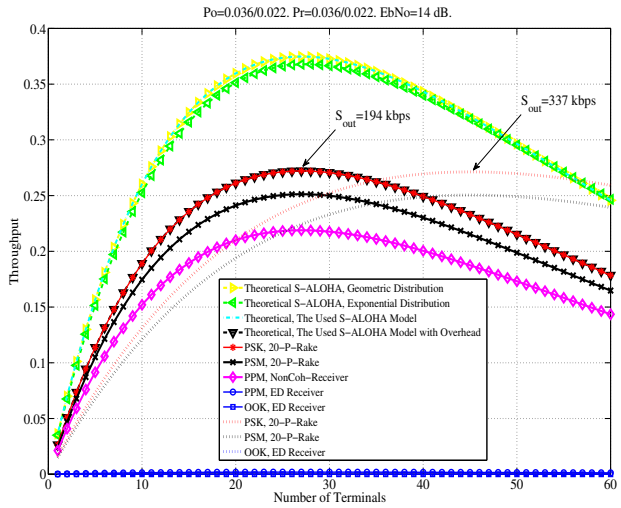

Figure 4. Throughput of S-ALOHA with different modulations.

the BER for the OOK-ED is significantly higher than the Reed-Solomon ability for decoding blocks and therefore neither of the receivers is producing significant throughput.

Another interesting result is the two dotted lines with peak values shifted right, approximately to 45 transmitting terminals. The red dotted line is the same 20 finger p-rake receiver with PSK as the red line with star marker and the black dotted line corresponds to the 20 finger p-rake receiver with PSM. The difference with these performance curves is that they are outputs from the system in which the PPM is bypassed and there are two bits (payload and MAC header bits) transmitted per one symbol interval. The outcome is that the maximum throughput of one terminal remains the same, but on a network level, due to the reduced number of transmitted symbols, this enables 74% increase on the successful volume of the traffic until reaching the maximum throughput.

Figure 5 presents the throughputs for different modulations as a function of number of terminals and as a function of E_b/N_0 in three dimensions. The effect of E_b/N_0 and the modulation method to the performance of communication system based on the IEEE Std. 802.15.4-2011 can now be clearly observed. When utilizing 20-finger p-rake with PSK, the throughput is slightly below 0.25 with E_b/N_0=10 dB, whereas other modulations' throughputs are zero. Maximum throughput of 0.28 is achieved with PSK when E_b/N_0=12 dB, while throughput of 20-finger p-rake PSM is still under 0.1 and furthermore, throughputs of the other modulations are zero. When E_b/N_0 is increased to 17 dB, all the other modulations but OOK-ED reaches the maximum throughput. Finally, when E_b/N_0=20 dB, also OOK-ED achieves close to the maximum throughput in the channel used. Another observation is when considering all the investigated receiver types, the E_b/N_0 "window" from zero-throughput to maximum throughput is approximately 3 dB. For example with PPM-ED, with E_b/N_0=14 dB, the throughput is zero and with E_b/N_0=17 dB, it reaches the maximum the system can have. This can be important information for system designers, when designing, for example, optimized power usage or placement of antennas.

5. CONCLUSIONS

In this paper, we implemented transceiver system models according to the IEEE Std. 802.15.4-2011 IR-UWB definitions.

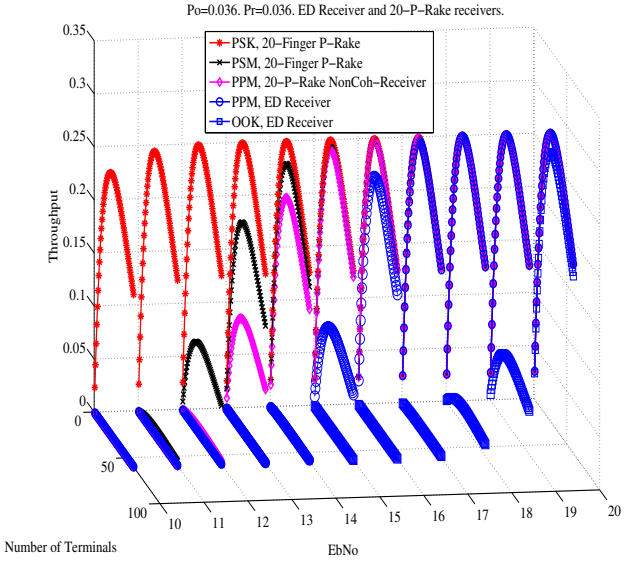

Figure 5. Throughput of S-ALOHA of different modulations and with different E_b/N_0 values.

We constructed the PHY system based on the novel modulation solutions and presented simulation results of different possible receiver structures that can be used based on the proposed solution. Additionally, we extended the inspections to MAC simulations to analyze the system level performance also.

It was also shown in system level inspections that different modulations and receiver structures affect significantly to the performance of a communication system based on IEEE Std. 802.15.4-2011. Based on the results, it can be clearly determined which E_b/N_0 value is required for sufficient BER level for different receivers in order to design practical device. In addition and the most important, we demonstrated the 74% increase on the successful volume of the traffic of the network by simply taking the intervals allocated for the PPM and using them both for data transmission.

Various impulse radio ultra wideband modulation combinations for increasing the data rate capacity have been reported in the literature over the years. Since the actual transmission, independent of the modulation used, is very similar in IR-UWB, it would be very useful to allow the usage of as many as possible of them in a single IR-UWB standard. This is possible within the current standard IR-UWB definitions of the both IEEE standards, in the 802.15.4-2011 and in the 802.15.6-2012. With a possibility to use different modulations for different purposes increases the adaptability of any system using IR-UWB. The applications for IR-UWB are already ranging quite a lot, from sensors in body area networks to sensors attached to portable devices for tracking purposes. Also the modulations have different advantages over different features. While binary PSK offers the best detection performance, OOK can provide very long battery life time. Therefore, in our opinion, it is justified to have a UWB standard with a pool of modulations to be chosen from, including the combinations of different modulations. By this way, at least, it provides opportunities for maximizing the data rate, maximizing the battery life time or performance of a receiver and offers flexible way for increasing the number of additional users.

Obviously it will need some general ruling, or mandatory modes for compatibility but similar procedures are implemented into the two published standards already.

6. ACKNOWLEDGMENTS

The work for this study was partly funded by Academy of Finland through project Dependable Wireless Healthcare Networks (DWHN) and by Finnish Funding for Innovation through project Enabling Future Wireless Healthcare System (EWiHS). First author has also received personal grants from Jenny ja Antti Wihurin rahasto, Riitta ja Jorma J. Takasen säätiö and Walter Ahlström Foundation.

7. REFERENCES

[1] IEEE Standard for Local and Metropolitan area networks - Part 15.4: Low-Rate Wireless Personal Area Networks (LR-WPANs), IEEE Std 802.15.4, 2011.

[2] IEEE Standard for Local and Metropolitan area networks - Part 15.6: Wireless Body Area Network, IEEE Std. 802.15.6, 2012.

[3] Niemelä, V, Hämäläinen, M., and Iinatti, J. 2011. Improved usage of time slots of the IEEE 802.15.4a UWB system model. In *Proc of the 2nd Int Workshop on Future Wellness and Medical ICT Systems in conjunction with the 14th Int Symp on Wireless Personal Multimedia Communication* (Brest, France, Oct. 3-7, 2011).

[4] Hoctor, R., and Tomlinson, H. 2002. Delay-hopped transmitted-reference RF communications. In *Proc of IEEE Conf on Ultra Wideband Systems and Technologies* (Baltimore, MD, USA, May 21-23, 2002), 265-269.

[5] Cui, S., Guan, Y.L., Teh, K.C., and Li, K.H. 2009. Pseudocoherent detection of OOK/PPM signals as zero-delay transmitted-reference signals with bandpass downsampling for UWB communications. *IEEE T Veh Technol* 58,8 (Oct, 2009), 4141-4148.

[6] Mitchell, C.J., Thadeu Freitas de Abreu, G., and Kohno, R. 2003. Combined pulse shape and pulse position modulation for high data rate transmission in ultra-wideband communications. *Int J Wireless Information Networks* 10,4 (Oct. 2003), 167-177.

[7] Ney da Silva, J.A, and de Campos, M.L.R 2003. Performance comparison of binary and quaternary UWB modulation schemes. In *Proc of IEEE Glob Telecomm conf* (San Francisco, USA, Dec. 1-5, 2003), 789-793.

[8] Majhi, S., Madhukumar, A.S., Premkumar, A.B., and Chin, F. 2007. Modulation schemes based on orthogonal pulses for time hopping ultra wideband radio systems. In *Proc. IEEE ICC* (Glasgow, Scotland, Jun. 24-28, 2007), 4185-4190.

[9] Liu, W., Zhou, Z., Bai, Z., Shen, H., Zhang, W., and Kwak, K.S. 2005. A novel UWB modulation method based on time-frequency energy distribution. In *Proc. IEEE Int Symp on Communications and Information Technology* (Beijing, China, Oct. 12-14, 2005), 960-963.

[10] Paso, T., Niemelä, V., Haapola, J., and Iinatti, J. 2012. Novel modulation adaptation techniques for IEEE 802.15.4a UWB system. In *Proc. the 6th Int Symp on Medical Information and Communication Technology* (La Jolla, California, USA, Mar. 25-29, 2012).

[11] Niemelä, V., Hämäläinen, M., and Iinatti, J. 2011. IEEE 802.15.4a UWB Receivers in medical applications. *Int. J. Ultra Wideband Communications and Systems* 2, 2 (2011), 73-82.

[12] Namislo, C. 1984. Analysis of mobile radio slotted aloha networks. *IEEE T Veh Technol* 33, 3 (Aug. 1984), 199-204.

[13] Hsieh, Y.-F., and Metzner, J.J. 1996. Comments on a widely used capture model for slotted aloha. *IEEE T Commun* 44, 4 (Apr. 1996), 419.

[14] Zhang, J., Orlik, P.V., Sahinoglu, Z., Molisch, A.F., Kinney, P. 2009. UWB systems for wireless sensor networks. In *Proc. of the IEEE* 97, 2 (Feb. 2009), 313-331.

[15] Karapistoli, E., Pavlidou, F.-N., Gragopoulus, I., and Tsetsinas, I. 2010. An overview of the IEEE 802.15.4a standard. *IEEE Commun Mag* 48, 1 (Jan. 2010), 47-53.

[16] Hämäläinen, M., Iinatti, J. 2014. Wireless UWB Body Area Networks: Using the IEEE802.15.4-2011. Academic Press.

[17] Taparugssanagorn, A., Pomalaza-Ráez, C., Isola, A., Tesi, R., Hämäläinen, M., and Iinatti, J. 2010. UWB channel modelling for wireless body area networks in a hospital. *Int. J. Ultra Wideband Communications and Systems* 1, 4 (2010), 226-236.

[18] Niemelä, V., Hämäläinen, M., Iinatti, J., and Taparugssanagorn, A. 2011. P-rake receivers in different measured WBAN hospital channels. In *The 5th Int Symp on Medical Information and Communication Technology* (Montreux, Switzerland, Mar. 27-30, 2011).

[19] Niemelä, V., Haapola, J., Hämäläinen, M., and Iinatti, J. 2012. Integration interval and threshold evaluation for an energy detector receiver with PPM and OOK modulations. In *The 7th Int Conf in Body Area Networks* (Oslo, Norway, Sep. 24-26, 2012).

[20] Kleinrock, L., and Lam, S.S. 1975. Packet switching in a multiaccess broadcast channel: performance evaluation. *IEEE T Commun* 23, 4 (April 1975), 410-423.

[21] Martelli, F., Goratti, L., and Haapola, J. 2010. Performance of sensor MAC protocols for medical ICT using IR-UWB. In *The 3rd Int HEALTHINF conf* (Valencia, Spain, Jan. 20-23, 2010).

[22] Arnon, S., Bhastekar, D., Kedar, D., and Tauber, A. 2003. A comparative study of wireless communication network configurations for medical applications. *IEEE Wirel Commun* 10, 1 (Feb. 2003), 56-61.

[23] Proakis, J.G. 2001. Digital Communications. 4th edition, McGraw-Hill Higher Education, 254-272.